

DMD #19885

The 'albumin effect' and *in vitro* – *in vivo* extrapolation: Sequestration of long chain unsaturated fatty acids enhances phenytoin hydroxylation by human liver microsomal and recombinant cytochrome P450 2C9

Andrew Rowland, David J Elliot, Kathleen M Knights, Peter I Mackenzie and John O Miners

Department of Clinical Pharmacology, Flinders University and Flinders Medical Centre, Bedford Park, Adelaide, Australia.

DMD #19885

Running Title: Mechanism for enhanced phenytoin hydroxylation by albumin

Corresponding author:

Professor John Miners
Department of Clinical Pharmacology
Flinders Medical Centre
Bedford Park
SA 5042
Australia

telephone 61-8-82044131
fax 61-8-82045114
email john.miners@flinders.edu.au

Manuscript details:

Number of text pages (including references and legends) – 32

Number of tables – 2

Number of figures – 4

Number of references – 40

Abstract – 250 words

Introduction – 656 words

Discussion – 1,475 words

Abbreviations:

BHT, butylated hydroxytoluene; BSA, bovine serum albumin; CYP, cytochrome P450; FA, fatty acid; FAME, fatty acid methyl ester; HLM, human liver microsomes; HSA, human serum albumin; HSA-FAF, essentially fatty acid free human serum albumin; OxR, NADPH cytochrome P450 oxidoreductase; PHY, phenytoin; HPPH, hydroxyphenytoin; TBA, 5-ethyl-5-*p*-tolylbarbituric acid.

DMD #19885

ABSTRACT

This study characterized the mechanism by which bovine serum albumin (BSA) reduces the K_m for phenytoin (PHY) hydroxylation, and the implications of the 'albumin effect' for *in vitro* – *in vivo* extrapolation of kinetic data for CYP2C9 substrates. BSA and fatty acid free human serum albumin (HSA-FAF) reduced the K_m values for PHY hydroxylation (based on unbound substrate concentration) by human liver microsomes (HLM) and recombinant CYP2C9 by approximately 75%, with only a minor effect on V_{max} . In contrast, crude HSA increased the K_m with both enzyme sources. Mass spectrometric analysis of incubations containing HLM was consistent with the hypothesis that BSA sequesters long chain unsaturated acids (arachidonic, linoleic, oleic) released from membranes. A mixture of arachidonic, linoleic and oleic acids, at a concentration corresponding to one twentieth of the content of HLM, doubled the K_m for PHY hydroxylation by CYP2C9, without affecting V_{max} . This effect was reversed by addition of BSA to incubations. K_i values for arachidonic acid inhibition of human liver microsomal- and CYP2C9- catalyzed PHY hydroxylation were 3.8 μ M and 1.6 μ M, respectively. Similar effects were observed with heptadecenoic acid, the most abundant long chain unsaturated acid present in *E. coli* membranes. Extrapolation of CL_{int} values for each enzyme source determined in the presence of BSA and HSA-FAF accurately predicted the known CL_{int} for PHY hydroxylation *in vivo*. The results indicate that previously determined *in vitro* K_m values for CYP2C9 substrates are almost certainly over-estimates, and accurate *in vitro* – *in vivo* extrapolation of kinetic data for CYP2C9 substrates is achievable.

DMD #19885

INTRODUCTION

The use of *in vitro* kinetic data to predict drug metabolic stability *in vivo* has attracted widespread interest, particularly in preclinical drug development. Most commonly, intrinsic clearance (CL_{int}) determined *in vitro* is scaled to an *in vivo* CL_{int} and hepatic clearance (CL_H) using human liver microsomes (HLM) or hepatocytes as the enzyme source (Houston 1994; Iwatsubo *et al.* 1997; Obach *et al.* 1997; McGinnity *et al.* 2004). Although *in vitro* models and scaling approaches have been progressively refined in recent years, *in vitro* – *in vivo* extrapolation (IV-IVE) typically results in under-prediction of *in vivo* CL_{int} and CL_H (and hence hepatic extraction ratio, E_H). With HLM as the enzyme source, *in vivo* CL_{int} is under-predicted by approximately an order of magnitude for drugs eliminated by either cytochrome P450 or UDP-glucuronosyltransferase catalyzed biotransformation (Boase and Miners 2002; Ito and Houston 2005). Prediction bias is improved using hepatocytes (Soars *et al.* 2002; Riley *et al.* 2005), but there remains an approximate 4-fold under-prediction of the *in vivo* CL_{int} (Miners *et al.* 2006; Brown *et al.* 2007).

The reason for the under-prediction of *in vivo* CL_{int} (and CL_H) based on human liver microsomal kinetic data remains unclear. Non-specific microsomal binding, variability in experimental conditions and physiological scaling factors, and inappropriate kinetic modelling all affect the reliability of *in vitro* – *in vivo* extrapolation (Miners *et al.* 2006), but significant under-prediction remains even when these factors are taken into account. Similarly, involvement of hepatic uptake transporters potentially accounts for the improved predictivity of kinetic data generated with hepatocytes, although recent data suggest that hepatic uptake is not rate-limiting in the clearance of lipophilic drugs (Doherty *et al.* 2006; Halifax and Houston 2006).

DMD #19885

The addition of bovine serum albumin (BSA) to incubations of HLM has been reported to increase the rate of metabolism of CYP2C9 substrates (Ludden *et al.* 1997; Carlile *et al.* 1999; Tang *et al.* 2002; Zhou *et al.* 2004) and microsomal CL_{int} values of UGT2B7 substrates (Uchaipichat *et al.* 2006; Rowland *et al.* 2007) substrates. After accounting for binding to albumin, K_m values for phenytoin (PHY) *p*-hydroxylation, tolbutamide tolymethylhydroxylation, and zidovudine glucuronidation by HLM in incubations supplemented with 2% BSA were 6- to 20- fold lower compared to K_m values generated in the absence of BSA. Maximal velocity was generally unaffected by BSA, although Carlile *et al.* (1999) reported a 2-fold reduction in the V_{max} for tolbutamide tolymethylhydroxylation.

Consistent with this observation, long chain unsaturated fatty acids, including oleic (C18:1*n*-9), linoleic (C18:2*n*-6) and arachidonic (C20:4*n*-6) acids, are known potent inhibitors of UGT2B7 (Tsoutsikos *et al.* 2004). We have demonstrated recently that BSA and fatty acid free human serum albumin (HSA-FAF) reduce the K_m for zidovudine glucuronidation by HLM and recombinant UGT2B7 (expressed in HEK293 cells) by sequestration of inhibitory long chain unsaturated fatty acids released from membranes during the course of an incubation (Rowland *et al.* 2007). CYP2C9 is known to catalyse the oxidation of C18:2*n*-6 and C20:4*n*-6 (Daikh *et al.* 1994; Rifkind *et al.* 1995; Draper and Hammock 2000) and, by analogy with UGT2B7, it might be speculated that the higher K_m values for microsomal PHY and tolbutamide hydroxylation observed in the absence of BSA arise from inhibition of CYP2C9 activity by long chain unsaturated fatty acids.

Thus, the aims of the present study were to: characterise the effects of BSA, HSA and HSA-FAF on the kinetics of PHY hydroxylation by HLM and CYP2C9; demonstrate inhibition of PHY hydroxylation by long chain unsaturated fatty acids, and reversal of fatty acid inhibition by albumin; and show that the presence of BSA in incubations

DMD #19885

abolishes the metabolism of long chain fatty acids released from HLM during the course of an incubation. The results are consistent with the hypothesis that the 'albumin effect' as it applies to CYP2C9 substrates results from sequestration of inhibitory fatty acids, and suggest that under appropriate experimental conditions HLM may be a suitable enzyme source for the generation of kinetic data for *in vitro* – *in vivo* extrapolation.

DMD #19885

MATERIALS AND METHODS

Phenytoin (PHY), 5-(4'-hydroxyphenyl)-5-phenylhydantoin (hydroxy phenytoin; HPPH), 5-ethyl-5-*p*-tolylbarbituric acid (TBA), butylated hydroxytoluene (BHT), bovine serum albumin ('crude' BSA, product number A7906), human serum albumin ('crude' HSA; product number A9511), essentially fatty acid free HSA (HSA-FAF; product number A1887), heptadecenoic acid (C17:1), linoleic acid (C18:2 n -6), oleic acid (C18:1 n -9) and arachidonic acid (C20:4 n -6) were purchased from Sigma Aldrich (Sydney, Australia). MS grade ethyl acetate and acetonitrile were used for MS-MS experiments. All other reagents and solvents were of analytical reagent grade.

HPLC was performed using an Agilent 1100 series instrument (Agilent Technologies, Sydney, Australia) comprising a quaternary solvent delivery module, autoinjector and UV-Vis detector. The column was maintained at 25°C. Mass spectral data were collected on a MDS Sciex 3200 Q-trap triple quadrupole mass spectrometer (Applied Biosystems, Forster City, CA).

Human liver microsomes and expression of CYP2C9

Pooled human liver microsomes were prepared by mixing equal protein amounts from five human livers (H07, H10, H12, H29 and H40), obtained from the human liver 'bank' of the Department of Clinical Pharmacology of Flinders University. Approval for the use of human liver tissue in xenobiotic metabolism studies was obtained from both the Clinical Investigation Committee of Flinders Medical Centre and from the donors' next-of-kin. Human liver microsomes (HLM) were prepared by differential centrifugation, as described by Bowalgaha *et al.* (2005).

DMD #19885

CYP2C9 and OxR cDNAs

N-Terminus modifications previously shown to promote high levels of bacterial expression of human P450s were made to the wild-type CYP2C9 cDNA as previously described (Boye *et al.* 2004). The CYP2C9 cDNA was modified for bacterial expression by replacing the second codon with GCT (codes for Ala), deleting codons 3-20, and adjusting codons 21 through 26 for bacterial codon bias. The 1803bp product (3' UTR included) was ligated into the pCWori(+) bacterial expression plasmid. pCW-CYP2C9 was transformed into DH5 α *E. coli* cells and colonies screened for the correct plasmid by restriction enzyme analysis. Plasmid DNA was purified and confirmed on both strands by sequencing (ABI Prism 3100). The cDNA coding for OxR consisted of the OmpA signal sequence fused upstream of the full length native rat OxR sequence (Boye *et al.* 2004). The rOxR expression construct was generated using the bacterial plasmid, pACYC.

Heterologous expression of pCW-CYP2C9 and pACYC-rOxR

pCW-CYP2C9 and pACYC-rOxR were separately transformed into DH5 α *E. coli* cells. Cells were cultured and *E.coli* membrane fractions separated using the method of Boye *et al.* (2004). CYP2C9 and OxR membrane fractions were mixed on ice to provide a CYP to OxR ratio of 1:5. A CYP2C9 to OxR ratio of 1:5 has been shown previously to result in optimal CYP2C9 activity (Boye *et al.* 2004). CYP2C9 expression was determined by carbon monoxide difference spectroscopy while the rate of cytochrome c reduction was used as a measure of the OxR activity of membrane fractions.

PHY hydroxylation assay

DMD #19885

Incubations, in a total volume of 500 μ L, contained phosphate buffer (0.1M, pH7.4), HLM (0.375mg), albumin (0 or 2%), and PHY (0.5-100 μ M). Following a 5min pre-incubation, reactions were initiated by the addition of NADPH regenerating system (1mM NADP, 10mM glucose 6-phosphate, 2IU/mL glucose 6-phosphate dehydrogenase and 5mM MgCl₂). Incubations were performed at 37°C in a shaking water bath for 45min. Reactions were terminated by the addition of perchloric acid (5 μ L, 70% v/v) and cooling on ice. After addition of TBA (10 μ M), the assay internal standard, incubation mixtures were transferred to 15mL culture tubes that contained sodium chloride (0.75 g) and extracted twice with 2mL of ethyl acetate. The combined extracts were evaporated to dryness under a stream of N₂. Metabolite and internal standard extraction efficiencies, determined by comparison to a standard curve from buffer, were greater than 95%. Residues were reconstituted in 0.1mL of the HPLC mobile phase and a 20 μ L aliquot was injected directly onto the HPLC column.

For reactions performed using recombinant CYP2C9, incubation mixtures contained *E. coli* expressed CYP2C9 (10pmolCYP/incubation; 0.02 mg/mL *E. coli* membrane protein) and OxR (50pmolOxR/incubation; 0.57mg/mL *E.coli* membrane protein) membranes in place of HLM protein, and the incubation time was increased to 90min. Under the reaction conditions employed PHY hydroxylation was linear with respect to incubation time and protein concentration to 90min and 1mg/mL, respectively, for HLM, and 120min and 20pmolCYP/incubation, respectively, for recombinant CYP2C9. PHY hydroxylation by untransformed *E. coli* membranes was not detectable.

Quantification of HPPH formation

HPPH formation was determined by HPLC. Analytes were separated on a Synergi Hydro RP analytical column (150 x 3.0mm 4 μ m, Phenomenex, Sydney, Australia) using a mobile phase comprising 70% 2mM triethylamine (pH adjusted to 2.5 with

DMD #19885

perchloric acid) and 30% acetonitrile, at a flow rate of 0.6mL/min. Column eluant was monitored by UV absorbance at 214nm. Retention times for HPPH, TBA and PHY were 4.3, 6.1 and 7.8min, respectively. HPPH formation was quantified by comparison of peak area ratios to those of a HPPH standard curve prepared over the concentration range 0.05 – 5 μ M. Overall within day assay reproducibility was assessed by measuring HPPH formation in 8 separate incubations of the same batch of pooled HLM. Coefficients of variation were 4.2% and 2.6% for PHY concentrations of 1 μ M and 50 μ M, respectively. The lower limit of quantitation (assessed as 3 times background noise) for HPPH was 0.01 μ M.

Quantification of the fatty acid content of *E. coli* membranes

The fatty acid content of *E. coli* membranes (1mg/mL) was determined using a modification of the gas-liquid chromatographic method of Folch *et al.* (1956), as described by Rowland *et al.* (2007).

Binding of PHY to albumin, HLM and *E. coli* membranes

Binding of PHY to HLM, *E. coli* membranes and mixtures of albumin (BSA, HSA or HSA-FAF; 2%) with each enzyme source was measured by equilibrium dialysis according to the method of McLure *et al.* (2000). Binding measurements were performed using a Dianorm equilibrium dialysis apparatus that comprised Teflon™ dialysis cells (capacity of 1.2mL per side) separated into two compartments with Sigma Aldrich dialysis membrane (molecular mass cut off 12kDa). One side of the dialysis cell was loaded with 1ml of PHY (1 to 50 μ M) in phosphate buffer (0.1M, pH 7.4). The other compartment was loaded with 1ml of either HLM in phosphate buffer (0.1M, pH 7.4), *E. coli* membranes in phosphate buffer (0.1M, pH 7.4), or a combination of albumin with each enzyme source in phosphate buffer (0.1M, pH 7.4).

DMD #19885

The dialysis cell assembly was immersed in a water bath maintained at 37°C and rotated at 12rpm for 4hr. Control experiments were also performed with phosphate buffer or albumin on both sides of the dialysis cells at low and high concentrations of PHY to ensure that equilibrium was attained. A 200µL aliquot was collected from each compartment, treated with ice-cold methanol containing 8% glacial acetic acid (200µL), and cooled on ice. Samples were subsequently centrifuged at 4,000g for 10min at 10°C and an aliquot of the supernatant fraction (5µL) was analysed by HPLC.

Quantification of PHY binding

Separation of PHY was achieved on a Waters NovaPak C₁₈ analytical column (3.9 x 150mm, 4µm, Waters, Sydney, Australia) using a mobile phase comprising 60% 2mM triethylamine (pH adjusted to 2.5 with perchloric acid) and 40% acetonitrile, at a flow rate of 1mL/min. Column eluant was monitored at 214nm. The retention time for PHY under these conditions was 2.8min. PHY concentrations in dialysis samples were determined by comparison of peak areas to those of a PHY standard curve prepared over the concentration range 0.25 to 50µM. Within day assay variability was assessed by measuring PHY (1 and 50µM; n=5 for each concentration) in samples containing phosphate buffer (0.1M, pH 7.4) or BSA in phosphate buffer (0.1M, pH 7.4). Coefficients of variation were less than 3% in all cases.

Mass spectrometric investigation of fatty acid binding to BSA

Incubation samples, (500µL), containing phosphate buffer (0.1M, pH7.4), HLM (0.375mg) and BSA (0 or 2%), were incubated using the conditions described for PHY hydroxylation (see above). Samples were acidified with glacial acetic acid then extracted with ethylacetate (2 x 0.3mL) containing BHT (20mg/L) by vortex mixing.

DMD #19885

Following centrifugation (13,000g, 4min), the combined organic extract was evaporated to dryness under vacuum and the residue redissolved in 1:1 acetonitrile-water (200 μ L). Mass spectra were obtained by direct infusion (10 μ L/min) into the electrospray ion source operated in negative ionization mode. The ionspray voltage was -3.5kV, declustering potential -75V and the ion source temperature was set at 300°C. Curtain gas and ion source gas flow were set at 10 and 30L/min, respectively. MS scans were collected in enhanced mode with a scan rate of 1000amu/s. Enhanced product ion scans were used to confirm peak identity with nitrogen as the collision gas.

Data analysis

Kinetic data are presented as the mean \pm standard deviation of four experiments with pooled HLM or recombinant CYP2C9. Kinetic constants for PHY hydroxylation by HLM and recombinant CYP2C9 in the presence and absence of albumin were generated by fitting experimental data to the Michaelis-Menten equation. Fitting was performed with EnzFitter (version 2.0.18.0; Biosoft, Cambridge, UK) based on the unbound substrate concentration present in incubations.

Intrinsic clearances (CL_{int}) for PHY hydroxylation by HLM and recombinant CYP2C9 were determined as V_{max}/K_m . Microsomal CL_{int} was converted to whole liver CL_{int} using scaling factors that correct for microsomal yield and liver weight using the equation:

$$CL_{int.liver} = \left[\frac{V_{max}(HLM)}{K_m(HLM)} \right] \times MPPGL \times LW$$

where V_{max} and K_m are the maximal velocity and Michaelis constant for the microsomal reaction, respectively; MPPGL is the mass of microsomes per gram of

DMD #19885

human liver tissue (taken as 38mg/g) and LW is the average weight of a human liver (1500g). The result was multiplied by 0.00006 to convert $\mu\text{L}/\text{min}$ to L/hr . The MPPGL value of 38mg/g corresponds to the geometric mean of the microsomal yield reported by Hakooz *et al.* (2006), and is in agreement with the mean MPPGL for the preparation of HLM from livers in the Flinders Medical Centre human liver 'bank' (JO Miners, unpublished data).

Similarly, CL_{int} determined for recombinant CYP2C9 was converted to whole liver CL_{int} using scaling factors that correct for CYP abundance per mg of microsomal tissue, microsomal yield and liver weight using the equation (Proctor *et al.* 2004):

$$\text{CL}_{\text{int.liver}} = \left[\frac{V_{\text{max}}(\text{rCYP}) \times \text{CYP}_{\text{abundance}}}{K_{\text{m}}(\text{rCYP})} \right] \times \text{MPPGL} \times \text{LW}$$

where V_{max} and K_{m} are the maximal velocity and the Michaelis constant for the recombinant CYP2C9 catalyzed reaction, respectively; $\text{CYP}_{\text{abundance}}$ is the abundance of CYP2C9 in 1g of human liver microsomes (73pmol; Rostami-Hodjegan and Tucker 2007); MPPGL and LW as described previously. Again, the result was multiplied by 0.00006 to express CL_{int} in L/hr .

In vivo CL_{int} values for PHY hydroxylation were calculated from area under the plasma concentration-time curve (AUC) data from four studies (Svensen *et al.* 1975; Gugler *et al.* 1976; Dickinson *et al.* 1985; Tassaneeyakul *et al.* 1992) using the equation:

$$\text{CL}_{\text{int}} = \frac{f_{\text{m}} \times \text{Dose}}{f_{\text{u,b}} \times \text{AUC}}$$

DMD #19885

where f_m is the fraction of the PHY dose converted to HPPH (0.79; Dickinson *et al.* 1985), dose is amount of drug administered (100-300mg as the sodium salt); $f_{u,b}$ is the fraction unbound in blood, calculated as the fraction unbound in plasma multiplied by the blood : plasma ratio (0.61; Kurata and Wilkinson 1974) and AUC is the area under the plasma concentration time curve. The mean *in vivo* CL_{int} from the four studies was determined to be 14.85L/hr

Statistical analysis (univariate General Linear Model, with Tukey post hoc analysis) was performed using SPSS for Windows, release 12.0.1, 2003 (SPSS Inc., Chicago, IL). Values of p less than 0.05 were significant.

DMD #19885

RESULTS

Binding of phenytoin to HLM, *E. coli* membranes and albumin

We have demonstrated that the sequestration of long chain unsaturated fatty acids released during the course of a microsomal incubation plateaus at BSA and HSA-FAF concentrations $\geq 1\%$ (Rowland et al., 2007), and previous reports of the effect of BSA on the kinetics of CYP2C9 substrates have typically employed a BSA concentration of 2% (Ludden et al., 1997; Carlile et al., 1999; Tang et al., 2002). Thus, an albumin (BSA, HSA, HSA-FAF) concentration of 2% was selected for investigation in the present study. The binding of PHY to HLM, *E. coli* membranes and albumin was calculated as the concentration of drug in the buffer compartment divided by the concentration of drug in the protein compartment and expressed as the fraction unbound in incubations ($f_{u,inc}$). Binding of PHY to pooled HLM and *E. coli* membranes was negligible ($<5\%$) across the PHY concentration range investigated (1 to 50 μ M), consistent with previous microsomal binding data from this laboratory (McLure et al. 2000). PHY bound to all forms of albumin. PHY binding was independent of concentration in the range 1 to 50 μ M, but varied with albumin form. The mean $f_{u,inc}$ values for PHY binding to mixtures comprising HLM (or *E. coli* membranes) with BSA, HSA and HSA-FAF (all 2%) were 0.27, 0.51 and 0.46, respectively. Where incubations contained albumin, the concentration of PHY present in reaction mixtures was corrected for binding in the calculation of kinetic parameters.

Effect of albumin on phenytoin hydroxylation by HLM and recombinant CYP2C9

Kinetic data for HPPH formation by human liver microsomal and *E. coli* expressed CYP2C9, in the presence and absence of albumin, was well modelled by the expression for the Michaelis-Menten equation. Kinetic parameters for PHY

DMD #19885

hydroxylation by pooled HLM and recombinant CYP2C9, in the presence and absence of BSA, HSA and HSA-FAF, are shown in Table 1. Respective K_m and V_{max} values for PHY hydroxylation by HLM and recombinant CYP2C9 in the absence of albumin were $20.8 \pm 1.5 \mu M$ and $17.8 \pm 0.3 \text{ pmol/min.mg}$, and $14.4 \pm 1.3 \mu M$ and $0.230 \pm 0.006 \text{ pmol/min.pmolCYP}$. These data are similar to previously reported kinetic parameters for PHY hydroxylation by HLM (Ludden *et al.* 1997; Carlile *et al.* 1999; Tang *et al.* 2002).

BSA (2%) and HSA-FAF (2%) increased the rate of PHY hydroxylation by both HLM and recombinant CYP2C9, predominantly by decreasing the K_m for this pathway, with a minor, but significant, effect on V_{max} (Figure 1 and Table 1). Mean K_m values for PHY hydroxylation by HLM and recombinant CYP2C9 were close in value (3.6-4.7 μM) for incubations conducted in the presence of BSA (2%) and HSA-FAF (2%). In contrast, crude HSA decreased the rate of PHY hydroxylation by HLM by increasing the K_m for this pathway without an effect on V_{max} (Table 1). Crude HSA was without effect on the kinetic parameters for PHY hydroxylation by recombinant CYP2C9.

Fatty acid content of *E. coli* membrane

The total concentration of C16 to C20 fatty acids released by hydrolysis of a suspension of *E. coli* membrane (1mg/mL) was $61 \mu M$, of which unsaturated fatty acids made up 42% (Table 2). Of the unsaturated fatty acids, heptadecenoic acid (C17:1), vaccenic acid (C18:1*n*-7) and linolenic acid (C18:3*n*-6) were observed in the highest concentrations. The fatty acid content of *E. coli* membrane is approximately 5-fold lower than the fatty acid content of HLM on a w/w basis (Rowland *et al.* 2007).

Detection of endogenous fatty acids and their hydroxylated metabolites released by enzyme sources in the presence and absence of BSA

DMD #19885

MS-MS product ion scans were used to confirm the identity of peaks at each m/z corresponding to the parent fatty acids or their oxygenated metabolites (Kerwin and Torvik 1996). Figure 2 shows the MS scans from incubations of pooled HLM with and without NADPH generating system and/or BSA. Both saturated (C16:0 and C18:0) and unsaturated (C18:1*n*-9, C18:2*n*-6 and C20:4*n*-6) long chain fatty acids were detected in incubations of HLM without generating system and BSA (Figure 2A). There was a greater than 50% reduction in the content of C18:0, C18:1*n*-9, C18:2*n*-6 and C20:4*n*-6 for incubations of HLM with NADPH generating system following incubation, and mono- hydroxylated metabolites of C16:0 and C18:1*n*-9 could be detected at m/z 271.3 and 297.3, respectively, with a dihydroxy metabolite of C18:2*n*-6 observed at m/z 311.2 (Figure 2B). Interestingly arachidonic acid was not observed following incubation with NADPH, presumably due to complete biotransformation. Unexpectedly however, oxygenated derivatives of arachidonic acid were also not detected, possibly as a result of fragmentation under the MS conditions employed. When BSA was included with NADPH generating system in the incubation mixture, the formation of hydroxylated metabolites of long chain fatty acids was almost abolished (Figure 2C). It should be noted that the presence of fatty acids arises from 'stripping off' fatty acids bound to BSA during extraction with ethyl acetate. Broadly similar observations were made for incubations with recombinant CYP2C9 in the absence and presence of NADPH generating system and/or BSA (data not shown)..

Inhibition of phenytoin hydroxylation by fatty acids in the presence and absence of albumin

Inhibition of PHY hydroxylation, at an added concentration of 5 or 15 μ M (the respective approximate K_m values in the presence and absence of albumin), by heptadecenoic acid (C17:1), oleic acid (C18:1*n*-9), linoleic acid (C18:2*n*-6) and

DMD #19885

arachidonic acid (C20:4*n*-6) was measured in the presence and absence of albumin using recombinant CYP2C9 as the enzyme source. When added at a concentration corresponding to 1/20th the known content in either HLM (C18:1*n*-9, C18:2*n*-6, C20:4*n*-6) or *E. coli* membranes (C17:1), each fatty acid inhibited PHY hydroxylation. The magnitude of inhibition increased with increasing degree of unsaturation; heptadecenoic (C17:1; 3μM), oleic (C18:1*n*-9; 3μM), linoleic (C18:2*n*-6; 3μM) and arachidonic (C20:4*n*-6; 1.5μM) acids inhibited PHY hydroxylation by 13, 22, 31 and 61%, respectively. In contrast, rates of PHY hydroxylation differed from the control values by <4% for incubations performed in the presence of BSA (2%).

The effect of a combination of fatty acids (comprising 3μM C18:1*n*-9, 3μM C18:2*n*-6 and 1.5μM C20:4*n*-6) on the kinetics of PHY hydroxylation by recombinant CYP2C9 was characterized in the presence and absence of BSA (2%). In the absence of BSA (2%), the combination of fatty acids caused a 2-fold increase in the K_m for PHY hydroxylation, from 14.4μM to 28.2μM, without a significant effect on V_{max} (0.246 versus 0.225pmol/min.pmolCYP) (Figure 3). In the presence of BSA (2%), the combination of fatty acids had no effect on the kinetics of PHY hydroxylation; respective K_m and V_{max} values in the presence and absence of the fatty acid mixture were 4.0 and 3.6μM and 0.242 and 0.246pmol/min.pmolCYP.

Kinetics of arachidonic and heptadecenoic acid inhibition of PHY hydroxylation by HLM and recombinant CYP2C9

Arachidonic and heptadecenoic acids inhibited PHY hydroxylation by human liver microsomal and *E. coli* expressed CYP2C9 in a competitive manner. The K_i values for arachidonic acid inhibition of HLM and *E. coli* expressed CYP2C9 were 3.8 and 1.6μM (Figure 4), respectively, while the K_i values for heptadecenoic acid inhibition of HLM and *E. coli* expressed CYP2C9 were 21.9 and 25.7μM, respectively.

DMD #19885

Prediction of phenytoin clearance based on kinetic values determined in the presence and absence of albumin

Predicted whole liver intrinsic clearance ($CL_{\text{int.liver}}$) values for PHY are shown in Table 1 for human liver microsomal and recombinant CYP2C9 kinetic data generated in the absence and presence of albumin. In the absence of albumin, the predicted $CL_{\text{int.liver}}$ values derived from incubations with HLM and recombinant CYP2C9 were $2.93 \pm 0.16\text{L/hr}$ and $4.01 \pm 0.24\text{L/hr}$, respectively. The use of kinetic data generated in the presence of BSA and HSA-FAF resulted in higher predicted $CL_{\text{int.liver}}$ values generated with HLM ($14.85 \pm 0.87\text{L/hr}$ and $15.39 \pm 0.32\text{L/hr}$, respectively) and recombinant CYP2C9 ($17.06 \pm 0.75\text{L/hr}$ and $15.36 \pm 0.43\text{L/hr}$, respectively) as the enzyme sources. The use of microsomal and recombinant CYP2C9 kinetic data obtained in the presence of BSA and HSA-FAF predict $CL_{\text{int.liver}}$ values that agreed well with the known *in vivo* mean CL_{int} for PHY of 14.85L/hr (data from: Svendsen *et al.* 1975; Gugler *et al.* 1976; Dickinson *et al.* 1985; Tassaneeyakul *et al.* 1992).

DMD #19885

DISCUSSION

The addition of BSA (2%) to incubations has previously been demonstrated to increase the rate of PHY hydroxylation by HLM (Ludden *et al.* 1997; Carlile *et al.* 1999; Tang *et al.* 2002; Zhou *et al.* 2004). More recently, we reported that BSA and HSA-FAF, but not 'crude' HSA, decreased the K_m values for zidovudine glucuronidation by approximately an order of magnitude, with both HLM and recombinant UGT2B7 (expressed in HEK293 cells) as the enzyme source (Rowland *et al.* 2007). The effect of BSA and HSA-FAF was concentration dependant between 0.05 to 1%, but plateaued from 1 to 4%. This work further showed that the mechanism of the 'albumin effect' involved sequestration of long chain unsaturated fatty acids (e.g. C18:1*n*-9, C18:2*n*-6 and C20:4*n*-6) that were released from the microsomal membrane during the course of an incubation and which acted as potent competitive inhibitors of UGT2B7 (Tsoutsikos *et al.* 2004; Rowland *et al.* 2007). The results of the present work similarly demonstrate that the decrease in the K_m for HPPH formation by both HLM and *E.coli* expressed CYP2C9 in the presence of BSA and HSA-FAF arises from sequestration of inhibitory long chain unsaturated fatty acids present in incubations. Importantly, kinetic parameters generated for HPPH formation by HLM and recombinant CYP2C9 in the presence of BSA and HSA-FAF accurately predicted PHY hepatic CL_{int} and CL_H *in vivo* indicating that this experimental system may be of value for IV-IVE for drugs cleared by cytochromes P450 and UDP-glucuronosyltransferase.

As in the previous investigation of zidovudine glucuronidation BSA and HSA-FAF, but not 'crude' HSA, decreased the K_m for HPPH formation by HLM and recombinant CYP2C9, from 20.8 to 4.7 μ M (HLM) and 14.4 to 3.6-4.1 μ M (CYP2C9) based on the unbound substrate concentration present in incubations. There was also a small, but statistically significant increase in V_{max} . The addition of 'crude' HSA to incubations

DMD #19885

either increased (HLM) or had no effect on the K_m for PHY hydroxylation. Crude HSA has significant amounts of bound long chain unsaturated fatty acids which limits further binding and may allow desorption of fatty acids into the incubation medium (Rowland *et al.* 2007).

C18:1n-9, C18:2n-6 and C20:4n-6 are amongst the most abundant long chain unsaturated fatty acids present (as phospholipids) in HLM (Waskell *et al.* 1982; Rowland *et al.* 2007). In contrast, the present work shows that heptadecenoic (C17:1) accounts for approximately 60% of the long chain unsaturated fatty acid content of *E.coli* membranes, with lower proportions of C18 and C20 unsaturated fatty acids. Consistent with the postulated inhibitory effect of fatty acids on CYP2C9 activity, addition of C17:1, C18:1n-9, C18:2n-6 and C20:4n-6 to incubations of *E.coli* expressed CYP2C9 at a concentration corresponding to approximately 1/20th of the known content of these fatty acids present in either HLM or *E.coli* membranes, decreased PHY hydroxylation activity due to an increase in K_m without a change in V_{max} , indicative of a competitive mechanism. Further experiments with C17:1 and C20:4n-6 confirmed that the individual fatty acids are competitive inhibitors of CYP2C9. K_i values for C20:4n-6 inhibition of PHY hydroxylation by HLM (3.8 μ M) and CYP2C9 (1.6 μ M) were lower than the K_i values for C17:1 (21.9 – 25.7 μ M). It should be noted that these values are almost certainly over-estimates since inhibition of PHY hydroxylation by long chain unsaturated fatty acids 'released' by the microsomal and *E.coli* membranes during the course of an incubation will occur simultaneously. In all cases, addition of BSA reversed the inhibition. The lower K_m value observed for incubations of recombinant CYP2C9 compared to HLM presumably reflects the lower content of inhibitory fatty acids in the expression system.

Mass spectral studies provided direct confirmatory evidence for a role of endogenous long chain unsaturated fatty acids in the inhibition of PHY hydroxylation by HLM.

DMD #19885

Several CYP enzymes, including CYP2C9, are known to oxidize long chain unsaturated fatty acids (Daikh *et al.* 1994; Rifkind *et al.* 1995; Draper and Hammock 2000). In the absence of NADPH generating system, molecular ions with m/z values corresponding to deprotonated C18:1 n -9, C18:2 n -6 and C20:4 n -6 were detected in incubations of HLM without exogenous substrate. Abundance of these ions increased during the course of an incubation (data not shown). Addition of NADPH generating system to incubation mixtures decreased the abundance of ions corresponding to the parent fatty acids and, in general, there was a corresponding increase in the content of mono- or di- hydroxylated metabolites. Further addition of BSA to incubations essentially abolished formation of the hydroxylated metabolites presumably since the sequestered long chain unsaturated fatty acids were not available for biotransformation. While the semi-quantitative nature of these experiments is acknowledged, the data are nevertheless consistent with the inhibition studies and with the previous observation that addition of BSA to incubations of HLM supplemented with UDP-glucuronic acid prevents the glucuronidation of endogenous long chain unsaturated fatty acids released during an incubation (Rowland *et al.* 2007).

AUC data from four studies (Svensen *et al.* 1975; Gugler *et al.* 1976; Dickinson *et al.* 1985; Tassaneeyakul *et al.* 1992) which employed single doses of PHY sodium (100-300mg) were used to calculate *in vivo* CL_{int} . The mean CL_{int} from the four studies was 14.85L/hr. Data from multiple dose studies was excluded to avoid the effect of autoinduction, as were data from studies that employed doses of ≥ 400 mg to ensure, as much as possible, that dosage was within the region of linear kinetics (Carlile *et al.* 1999). CL_{int} values generated with HLM and recombinant CYP2C9 in the absence of albumin under-predicted $CL_{int,liver}$ 4- to 5- fold. In contrast, kinetic data generated with HLM and recombinant CYP2C9 in the presence of BSA or HSA-FAF predicted mean $CL_{int,liver}$ within $\pm 15\%$ (Table 1), with exact correspondence of the extrapolated human

DMD #19885

liver microsomal CL_{int} obtained from incubations containing BSA. As alluded to above, however, the saturable kinetics of PHY in vivo may impact on the accuracy of IV-IVE for this substrate.

The K_m for PHY hydroxylation by human hepatocytes appears not to have been determined. However, as with K_m and K_i values generated for UGT2B7 substrates and inhibitors (Uchaipichat *et al.* 2006; Rowland *et al.* 2006 and 2007), available data indicate that the K_m 's for PHY hydroxylation obtained with HLM and recombinant CYP2C9 in the presence of BSA and HSA-FAF (viz. 3.6-4.7 μ M) reflect hepatocellular K_m . The mean *in vivo* unbound K_m for PHY hydroxylation is 3.4 μ M (discussed in Carlile *et al.* 1999).

The effect of BSA (2%) on $CL_{int.liver}$ prediction for PHY has been investigated previously by Carlile *et al.* (1999). These authors reported that the presence of BSA in incubations improved predictivity, but mean $CL_{int.liver}$ was underestimated by approximately 50%. It is noteworthy that V_{max} values reported by Carlile *et al.* (1999) are somewhat lower than those determined here and by Ludden *et al.* (1997). The effects of BSA and HSA-FAF on the kinetics of tolbutamide metabolism, another CYP2C9 substrate (Miners *et al.* 1988), have also been investigated. Carlile *et al.* (1999) reported that BSA (2%) increased the microsomal CL_{int} almost 6-fold, arising from a 20-fold reduction in mean K_m but halving of V_{max} . The higher microsomal CL_{int} generated in the presence of BSA tended to over-estimate $CL_{int.liver}$. However, the study of Carlile *et al.* (1999) included a very limited number of substrate concentrations, especially at concentrations below K_m . In contrast, Wang *et al.* (2002) reported that the inclusion of HSA-FAF (0.5%) in microsomal incubations only halved the K_m for tolbutamide hydroxylation (without affecting V_{max}), with remaining underprediction of $CL_{int.liver}$. The relatively low HSA-FAF concentration employed by Wang *et al.* (2002) may be sub-optimal for complete fatty acid sequestration. Further

DMD #19885

work with tolbutamide under standardized experimental conditions are warranted to resolve these differences. In this regard, studies are underway with a range of P450 substrates to determine the universality of the 'albumin' effect and to identify alternative fatty acid sequestering agents to albumin, given the current requirement to measure unbound fraction in incubations.

Metabolism by CYP2C9 is the primary clearance mechanism for a large number of clinically used drugs (Miners and Birkett, 1998). The kinetics of most CYP2C9 substrates have been characterized *in vitro*, with HLM and/or recombinant CYP2C9 as the enzyme source. Based on the effects of BSA and HSA-FAF on PHY and tolbutamide hydroxylation, published K_m values for CYP2C9 substrates are likely to be over-estimations. Taken together with the recently published data for UGT2B7 substrates and inhibitors (Uchaipichat *et al.* 2006; Rowland *et al.* 2006 and 2007), the present study further suggests that the addition of BSA or HSA-FAF to incubations of HLM and recombinant expression systems is likely to decrease the K_m values for substrates of any CYP or UGT enzyme inhibited by unsaturated long chain fatty acids. In turn, wherever metabolism involves an enzyme inhibitable by unsaturated long chain fatty acids it would be expected that prediction of both *in vivo* CL_{int} (or CL_H) is likely to be significantly improved when kinetic data are generated in the presence of BSA or HSA-FAF.

DMD #19885

ACKNOWLEDGEMENTS

Assistance from B. Lewis in providing recombinant CYP2C9 and OxR and K. Murphy for the analysis of the fatty acid content of *E.coli* membranes is gratefully acknowledged.

DMD #19885

REFERENCES

Boase S, Miners JO (2002). *In vitro* – *in vivo* correlations for drugs eliminated by glucuronidation: investigation with the model substrate zidovudine. *Br J Clin Pharmacol*, 54: 493-503.

Bowalgaha K, Elliot DJ, Mackenzie PI, Knights KM, Swedmark S, Miners JO (2005). Naproxen and desmethylnaproxen glucuronidation by human liver microsomes and recombinant human UDP-glucuronosyltransferases (UGT): Role of UGT2B7 in the elimination of naproxen. *Br J Clin Pharmacol*, 60: 423-433.

Boye SL, Kerdpin O, Elliot DJ, Miners JO, Kelly L, McKinnon RA, Bhasker CR, Yoovathaworn K, Birkett DJ (2004). Optimizing bacterial expression of catalytically active human cytochromes P450: comparison of CYP2C8 and CYP2C9. *Xenobiotica*. 34(1): 49-60.

Brown HS, Griffin M, Houston JB (2007). Evaluation of cryopreserved human hepatocytes as an alternative *in vitro* system to microsomes for prediction of metabolic clearance. *Drug Metab Dispos*, 35: 293–301.

Carlile DJ, Hakooz N, Bayliss MK, Houston JB (1999). Microsomal prediction of *in vivo* clearance of CYP2C9 substrates in humans. *Br J Clin Pharmacol*, 47: 625-635.

Daikh BE, Lasker JM, Raucy JL, Koop DR (1994). Regio- and stereoselective epoxidation of arachidonic acid by human cytochromes P450 2C8 and 2C9. *J Pharmacol Exp Ther*, 271(3):1427-33.

DMD #19885

Dickinson RG, Hooper WD, Patterson M, Eadie MJ, Maguire B (1985). Extent of urinary excretion of p-hydroxyphenytoin in healthy subjects given phenytoin. *Ther Drug Monit.* 7: 283-289.

Doherty MM, Poon K, Tsang C, Pang KS (2006). Transport is not rate-limiting in morphine glucuronidation in the single-pass perfused rat liver preparation. *J Pharmacol Exp Ther*, 317: 890-900.

Draper AJ, Hammock BD (2000). Identification of CYP2C9 as a human liver microsomal linoleic acid epoxygenase. *Arch Biochem Biophys*, 376: 199-205.

Folch J, Lees M, Stanley GHS (1956). A simple method for the isolation and purification of total lipids from animal tissue. *J Biol Chem*, 226: 497-509.

Gugler R, Manion CV, Azarnoff DL (1976). Phenytoin: Pharmacokinetics and bioavailability. *Clin Pharmacol Ther.* 19: 135–142.

Hakooz N, Ito K, Rawden H, Gill H, Lemmers L, Boobis AR, Edwards RJ, Carlile DJ, Lake BJ, Houston JB (2006). Determination of a human hepatic microsomal scaling factor for predicting in vivo drug clearance. *Pharm Res*, 23: 533-539.

Halifax D, Houston JB (2006) Uptake and intracellular binding of lipophilic amine drugs by isolated rat hepatocytes and implications for prediction of in vivo metabolic clearance. *Drug Metab Dispos*, 34: 1829-1836.

Houston JB (1994). Utility of in vitro drug metabolism data in predicting in vivo metabolic clearance. *Biochem Pharmacol*, 47: 1469–1479.

DMD #19885

Ito K, Houston JB (2005). Prediction of human drug clearance from in vitro and preclinical data using physiologically based and empirical approaches. *Pharm Res*, 22: 103-112.

Iwatsubo T, Hirota N, Ooie T, Suzuki H, Shimada N, Chiba K, Ishizaki T, Green CE, Tyson CA, Sugiyama Y (1997). Prediction of in vivo drug metabolism in the human liver from in vitro metabolism data. *Pharmacol Ther*, 73:147-171.

Kerwin JL, Torvik JJ (1996). Identification of monohydroxy fatty acids by electrospray mass spectrometry and tandem mass spectrometry. *Anal Biochem*, 237, 56-64.

Kurata D, Wilkinson GR (1974). Erythrocyte uptake and plasma binding of diphenylhydantoin. *Clin Pharmacol Ther*. 16: 355-362.

Ludden LK, Ludden TM, Collins JM, Pentikis HS, Strong JM (1997). Effect of albumin on estimations, *in vitro*, of phenytoin Vmax and Km values; implications for clinical correlation. *J Pharmacol Exp Ther*, 282: 391-396.

McGinnity DF, Soars MG, Urbanowicz RA, Riley RJ (2005). Evaluation of fresh and cryopreserved hepatocytes as in vitro drug metabolism tools for the prediction of metabolic clearance. *Drug Metab Dispos*, 32: 1247-1253.

McLure JA, Miners JO, Birkett DJ (2000). Non-specific binding of drugs to human liver microsomes. *Br J Clin Pharmacol*, 49: 453-461.

Miners JO, Smith KJ, Robson RA, McManus ME, Veronese ME, Birkett DJ (1988). Tolbutamide hydroxylation by human liver microsomes. Kinetic characterisation and

DMD #19885

relationship to other cytochrome P-450 dependent xenobiotic oxidations. *Biochem Pharmacol.* 37(6):1137-44

Miners JO, Birkett DJ (1998). Cytochrome P4502C9: an enzyme of major importance in human drug metabolism. *Br J Clin Pharmacol.* 45: 525-538.

Miners JO, Knights KM, Houston JB, Mackenzie PI (2006). In vitro-in vivo correlation for drugs and other compounds eliminated by glucuronidation in humans: pitfalls and promises. *Biochem Pharmacol*, 71: 1531-1539.

Obach RS, Baxter JG, Liston TE, Silber BM, Jones BC, MacIntyre F, Rance DJ, Wastall P (1997). The prediction of human pharmacokinetic parameters from preclinical and in vitro metabolism data. *J Pharmacol Exp Ther*, 283: 46-58.

Proctor NJ, Tucker GT, Rostami-Hodjegan A (2004). Predicting drug clearance from recombinantly expressed CYPs: intersystem extrapolation factors. *Xenobiotica*, 34: 151-178.

Rifkind AB, Lee C, Chang TK, Waxman DJ (1995) Arachidonic acid metabolism by human cytochrome P450s 2C8, 2C9, 2E1, and 1A2: regioselective oxygenation and evidence for a role for CYP2C enzymes in arachidonic acid epoxygenation in human liver microsomes. *Arch Biochem Biophys.* 320: 380-389.

Riley RJ, McGinnity DF, Austin RP (2005). A unified model for predicting human hepatic, metabolic clearance from in vitro intrinsic clearance data in hepatocytes and microsomes. *Drug Metab Dispos*, 33: 1304-1311.

DMD #19885

Rostami-Hodjegan A, Tucker 2007 GT (2007). Simulation and prediction of in vivo drug metabolism in human populations from in vitro data. *Nat Rev Drug Discovery*, 6: 140-148.

Rowland A, Elliot DJ, Williams JA, Mackenzie PI, Dickinson RG, Miners JO (2006). In vitro characterisation of lamotrigine N2-glucuronidation and the lamotrigine - valproic acid interaction. *Drug Metab Dispos*, 34: 1055-1062.

Rowland A, Gaganis P, Elliot DJ, Mackenzie PI, Knights KM, Miners JO (2007). Binding of inhibitory fatty acids is responsible for the enhancement of UDP Glucuronosyltransferase 2B7 activity by albumin: Implications for in vitro - in vivo extrapolation. *J Pharmacol Exp Ther*, 321: 137-147.

Soars MG, Burchell B, Riley RJ (2002). *In vitro* analysis of human drug glucuronidation and prediction of *in vivo* metabolic clearance. *J Pharmacol Exp Ther*, 301: 382-390.

Svensden TL, Kristensen MB, Hansen JM, Skovsted L (1975). The influence of disulfiram on the half life and metabolic clearance rate of diphenylhydantoin and tolbutamide in man. *Eur J Clin Pharmacol*. 9: 439-441.

Tang C, Lin Y, Rodrigues AD, Lin JH (2002). Effect of albumin on phenytoin and tolbutamide metabolism in human liver microsomes: an impact more than protein binding. *Drug Metab Dispos*, 30: 648-654.

Tassaneeyakul W, Veronese ME, Birkett DJ, Doecke CJ, McManus ME, Sansom LN Miners JO (1992). Co-regulation of phenytoin and tolbutamide metabolism in humans. *Br J Clin Pharmacol*. 34: 494-498.

DMD #19885

Tsoutsikos P, Miners JO, Stapleton A, Thomas A, Sallustio BC, Knights KM (2004). Evidence that unsaturated fatty acids are potent inhibitors of renal UDPglucuronosyltransferases (UGT): kinetic studies using human kidney cortical microsomes and recombinant UGT1A9 and UGT2B7. *Biochem Pharmacol*, 67: 191-199.

Uchaipichat V, Winner LK, Mackenzie PI, Elliot DJ, Williams JA, Miners JO (2006). Quantitative prediction of *in vivo* inhibitory drug interactions involving glucuronidated drugs from *in vitro* data: The effect of fluconazole on zidovudine glucuronidation. *Br J Clin Pharmacol*, 61: 427-439.

Wang J-S, Wen X, Backman JT, Neuvonen PJ (2002) Effect of albumin and cytosol on enzyme kinetics of tolbutamide hydroxylation and inhibition of CYP2C9 by gemfibrozil in human liver microsomes. *J Pharmacol Exp Ther*, 302 : 43-49.

Waskell L, Koblin D, and Canova-Davis E (1982) The lipid composition of human liver microsomes. *Lipids* 17:317-320

Zhou Q, Matsumoto S, Ding LR, Fischer NE, Inaba T (2004). The comparative interaction of human and bovine serum albumins with CYP2C9 in human liver microsomes. *Life Sci*, 75: 2145-2155.

DMD #19885

FOOTNOTES

This work was funded by a grant from the National Health and Medical Research Council of Australia. A.R. is the recipient of a Flinders University Research Scholarship.

DMD #19885

FIGURES

Figure 1 – Eadie-Hofstee plots ($V/[S]$ versus $[S]$) for PHY hydroxylation by HLM and recombinant CYP2C9 in the presence and absence of albumins. Points are experimentally determined values, whereas lines are from model fitting.

Figure 2 – Mass spectra demonstrating the presence of molecular ions corresponding to saturated and unsaturated long chain fatty acids (A, B and C), and mono-hydroxylated and di-hydroxylated metabolites of long chain unsaturated fatty acids (B). Incubation mixtures contained HLM: (A) without NADPH generating system and BSA, (B) with NADPH generating system, and (C) with NADPH generating system and BSA (2%).

Figure 3 – Kinetic plots (V versus $[S]$) for PHY hydroxylation by recombinant CYP2C9 in the presence and absence of a fatty acid mixture, with and without added BSA. Points are experimentally determined values, whereas curves are from model fitting.

Figure 4 – Dixon plot ($1/V$ versus $[I]$) for inhibition of recombinant CYP2C9 catalysed PHY hydroxylation by arachidonic acid. Points are experimentally determined values, whereas lines are from model fitting.

DMD #19885

Table 1 – Kinetics of phenytoin hydroxylation by HLM and *E. coli* expressed CYP2C9, in the presence and absence of 2% albumin

Enzyme source	Parameter	No albumin	BSA	HSA-FAF	HSA
HLM	K_m	20.8 ± 1.5	4.7 ± 0.3*	4.7 ± 0.2*	26.5 ± 1.0*
	V_{max}	17.8 ± 0.3	20.2 ± 0.5*	20.7 ± 0.8*	17.4 ± 0.3
	CL_{int}	0.86 ± 0.05	4.3 ± 0.3*	4.5 ± 0.1*	0.66 ± 0.02*
	$CL_{int.liver}$	2.93 ± 0.16	14.85 ± 0.87*	15.39 ± 0.32*	2.25 ± 0.07*
CYP2C9	K_m	14.4 ± 1.3	3.6 ± 0.2*	4.1 ± 0.2*	14.7 ± 0.1
	V_{max}	0.230 ± 0.006	0.246 ± 0.001*	0.249 ± 0.004*	0.236 ± 0.003
	CL_{int}	1.17 ± 0.07	4.99 ± 0.22*	4.49 ± 0.13*	1.17 ± 0.02
	$CL_{int.liver}$	4.01 ± 0.24	17.06 ± 0.75*	15.36 ± 0.43*	3.99 ± 0.06

Units: HLM: K_m , μM ; V_{max} , pmol/min/mg; CL_{int} , $\mu L/min/mg$. *E. coli* expressed CYP2C9:

K_m , μM ; V_{max} , pmol/min/pmolCYP; CL_{int} , $\mu L/min/mg$. $CL_{int.liver}$, L/hr.

* Significantly different ($P < 0.05$) from control value (determined in absence of albumin)

DMD #19885

Table 2 – Content of unsaturated C16 to C20 series fatty acids in *E. coli* membranes

Fatty acid	Molecular Weight	Amount present in <i>E.coli</i> membranes ^a
16:1 <i>n</i> -9	254.4	0.18
16:1 <i>n</i> -7	254.4	1.84
17:1	268.5	14.60
18:1 <i>n</i> -9	282.5	0.19
18:1 <i>n</i> -7	282.5	3.32
19:1	296.5	0.00
20:1 <i>n</i> -11	310.5	0.00
20:1 <i>n</i> -9	310.5	0.00
18:2 <i>n</i> -9	280.4	0.66
20:2 <i>n</i> -9	308.5	0.15
20:3 <i>n</i> -9	306.5	0.00
18:2 <i>n</i> -6	280.4	0.02
18:3 <i>n</i> -6	278.4	3.36
20:2 <i>n</i> -6	308.5	0.00
20:3 <i>n</i> -6	306.5	0.00
20:4 <i>n</i> -6	304.5	0.01
16:2 <i>n</i> -3	256.4	0.14
18:3 <i>n</i> -3	278.4	0.03
18:4 <i>n</i> -3	276.4	0.00
20:3 <i>n</i> -3	306.5	0.02
20:5 <i>n</i> -3	302.5	0.00

^a Units for fatty acid content are micromolar for a 1mg/mL suspension of *E.coli* membrane.

Figure 1

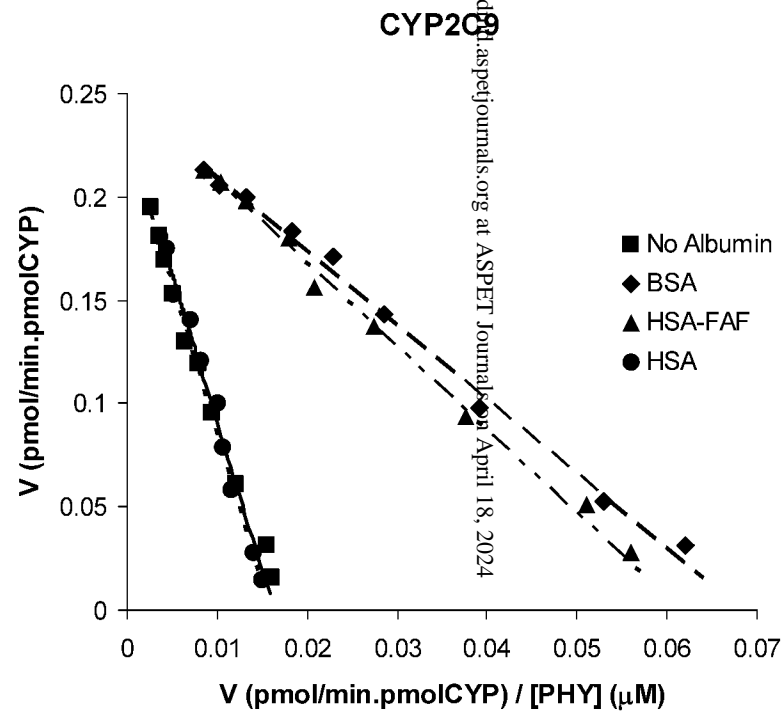
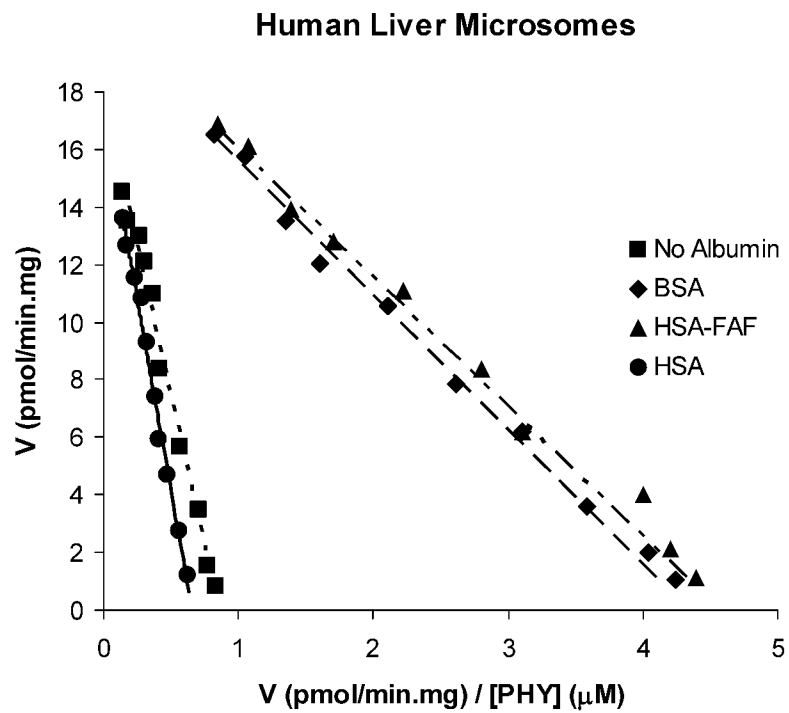


Figure 2

DMD Fast Forward. Published on February 6, 2008 as DOI: 10.1124/dmd.107.019885
This article has been copyedited and formatted for publication. The final version may differ from this version.

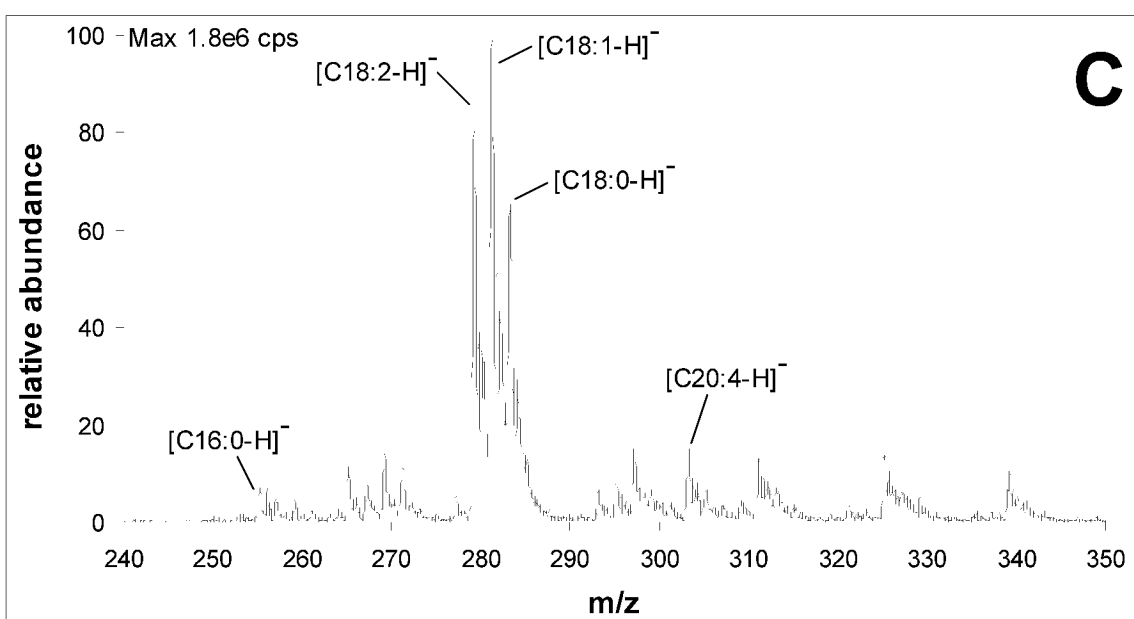
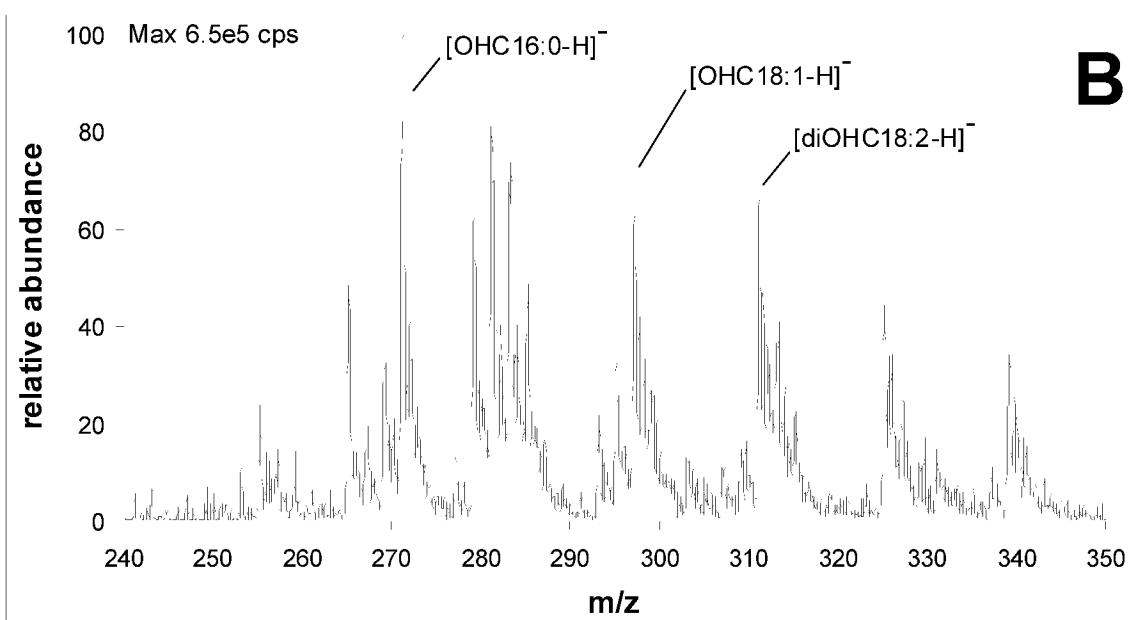
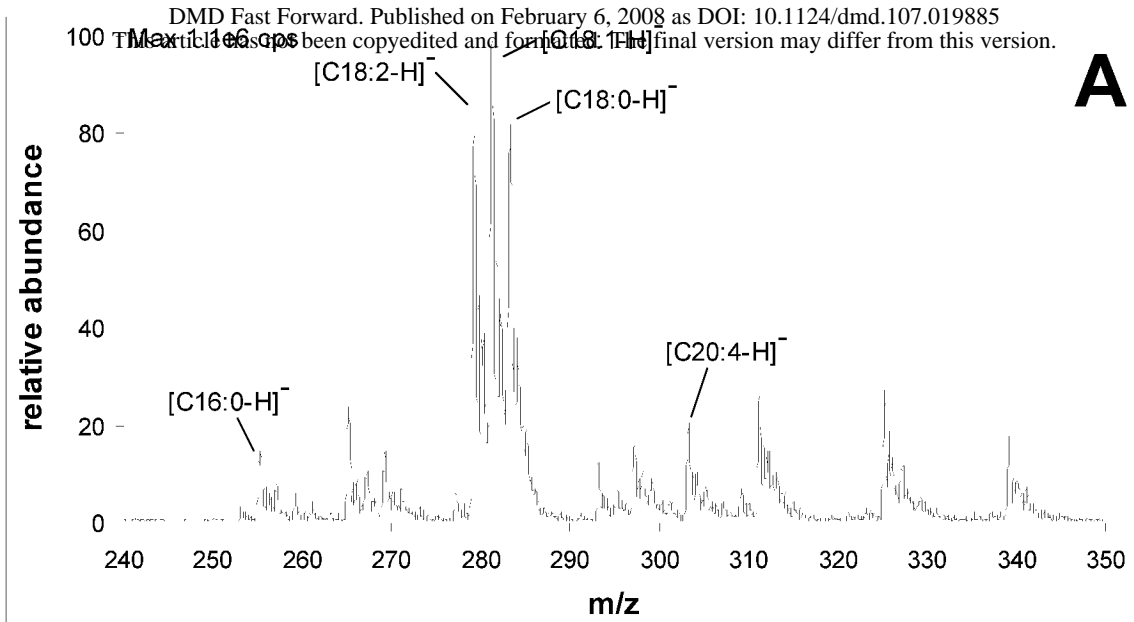
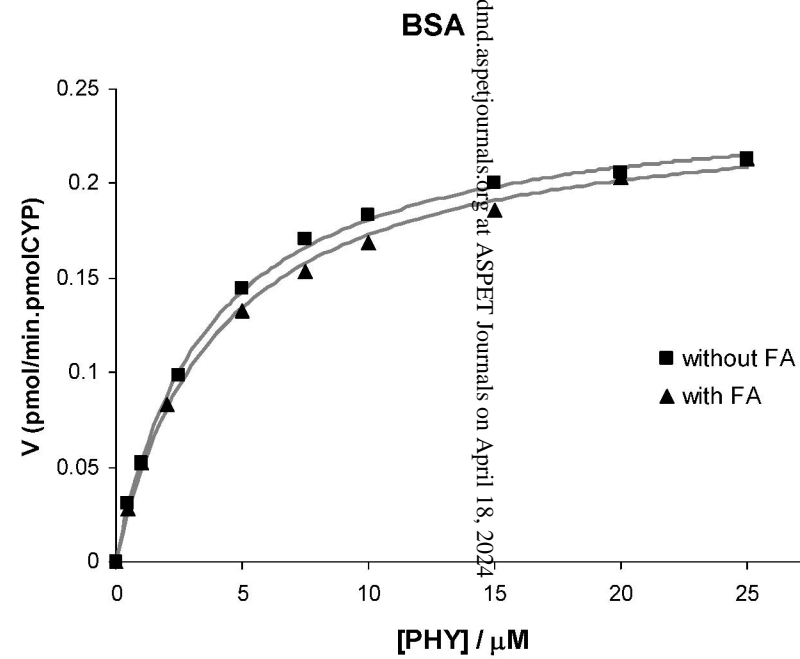
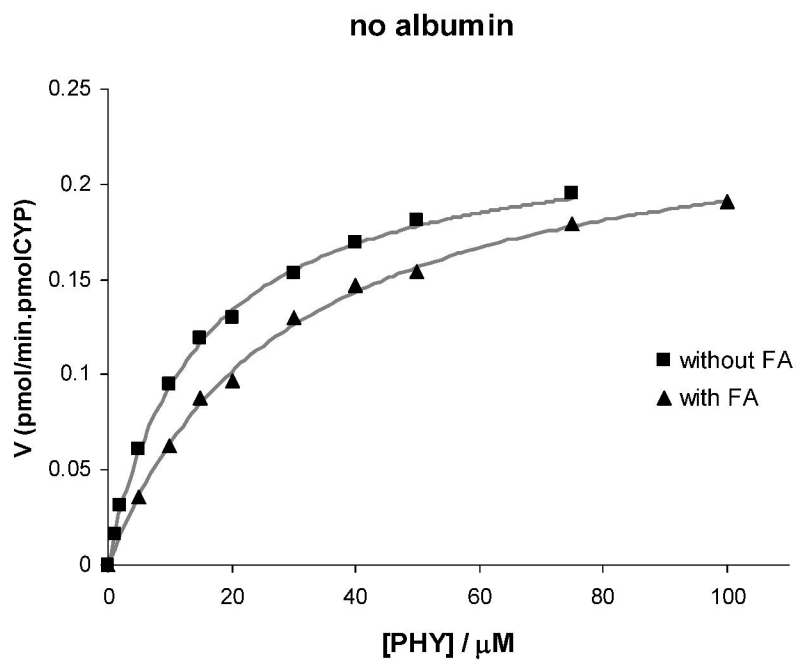


Figure 3



Downloaded from dnd.aspejournals.org at ASPET Journals on April 18, 2024

Figure 4

